# Flowfield simulation and aerodynamic performance analysis of complex iced aerofoils with hybrid multi-block grid

**Yihua Cao**[1]*, **Ke Chen**[1], and **J Sheridan**[2]

[1]Institute of Aircraft Design, Beijing University of Aeronautics and Astronautics, Beijing, People's Republic of China

[2]Department of Mechanical Engineering, Faculty of Engineering, Monash University, Victoria, Australia

*The manuscript was received on 5 September 2007 and was accepted after revision for publication on 2 January 2008.*

DOI: 10.1243/09544100JAERO286

**Abstract:** Flowfield simulation and aerodynamic performance analysis of complex iced aerofoil are conducted with hybrid multi-block grid technique. To overcome the difficulty of generating structure grid on complex geometry, a point-to-point hybrid grid generation method is developed in this paper. An unstructured grid is imposed in the zone near the iced aerofoil to handle the complicated iced geometry. A structure grid is imposed in the zone wrapping the unstructured grid to save the storage and computational time. The implementation of point-to-point hybrid grid simplifies the flux construction at the interface between two types of grid. The Reynolds-averaged Navier–Stokes equations are solved with implementation of the shear-stress transport two-equation turbulence model in both types of grid. As a comparison, the numerical simulation results with Spalart–Allmaras turbulence model are also presented. The results of numerical simulation on iced aerofoil validate the method developed in this paper and show that ice accretion has serious effect on aerodynamic performance of aerofoil.

**Keywords:** structure/unstructured hybrid grid, grid generation, ice accretion, aerodynamic performances, turbulence model, computational fluid dynamics

## 1 INTRODUCTION

Ice accretion on the leading edge of aircraft wing in flight will seriously affect the aerodynamic performances of aircraft and damage the flight safety, especially in taking off and landing. It has caused serious accidents in the history of civil aviation. Currently, there are two major fields in icing research. The first one is icing effect, which studies the flow field characteristics around the aircraft and degradation of aircraft performance due to the ice accretion. The other one is ice accretion, which studies the process of ice accretion, especially the growth of ice shape, in given flight and meteorological conditions.

The effects of ice accretion on aircraft can be studied through wind-tunnel experiments, flight tests, and computational simulation. With the development of computational fluid dynamics (CFD) technology, more and more researchers use the CFD tools in icing study. The most important steps in successful analysis on the effects of iced aerofoil with CFD are geometry preparation and grid generation. As for rime ice, which has simple figuration, there are no much more difficulties in structure grid generation. However, the complex glaze ice has horns and feather surface, which make it very difficult to generate structure grid, especially high quality structure grid. To generate high quality structure grid, many researchers developed various methods and tools to overcome the problems described above. Chi *et al.* [**1**] presented a number of grid generation methods to construct high quality single- and multi-block structure grid for complex ice shapes, such as NLF0414 aerofoil with the 623 ice shape. And the NASA Glenn's Smaggice 2D [**2**], a software toolkit used to handle the geometry of

**Corresponding author: Institute of Aircraft Design, Beijing University of Aeronautics and Astronautics, 37 Xueyuan Road, Haidian District, Beijing 100083, People's Republic of China. email: yihuacs@yahoo.com.cn*

icing aerofoil and grid generation, was developed to overcome the difficulties of implementing CFD flow solvers in icing research, especially in grid generation. However, the methods developed by Chi *et al.* need to decide the blocking topology at first, which is experiential and time-consuming. And the toolkit, Smaggice 2D, is not available for the researchers outside USA and may lose some surface characteristics at some conditions.

In this paper, a structure/unstructured hybrid grid generation method is developed to avoid generating structure grid in the whole computational field. The most complex iced shape, 145-m glaze ice of commercial transport jet main aerofoil (B757/767), is selected to validate the method. The iced shape includes not only the horns of glaze ice, but also the feather surface of rime ice. The detail geometry of 145-m glaze ice can be found in reference [**3**]. It is very difficult to generate high quality single- and multi-block structure grid on such iced aerofoil. In this study, an unstructured grid is used to handle the boundary of complex ice shape, and a structure grid is wrapping around the unstructured grid with point-to-point type boundary at the interface of two types of grid. The flow field around the aerofoil is gained by solving Navier–Stokes equations with the implement of a two-equation turbulence model.

## 2 GRID GENERATION

When structure grid is used in ice accretion study, there are two main issues need to be focused on. The first one is the surface preparation. Because the geometry of glaze ice aerofoil is composed of not only protruding horns and feathers but also small-scale surface roughness, the surface preparation is very important to aerodynamics performance prediction. The second one is blocking topology. Two types of blocking strategy are used in generally, single-block and multi-block. Each of them has its merit and shortage. The single-block grid is difficult to generate in some situations and the quality is hard to handle. The multi-block grid is bothering in topology definition and the clustered grid line at the block boundary is not easy to control. Though high-quality single- and multi-block grids can be generated with the grid generation and blocking techniques developed by Chi *et al.* [**1**] and Zhu *et al.* [**4**], local elliptic smoothing and variable thickness wrap-around grids are required for both single- and multi-block grids. And some research results can be found in reference [**5**].

The NASA Glenn's Smaggice 2D is widely used to prepare the surface geometry of iced aerofoil and to generate the structure computation grid. The software toolkit uses smoothing routines to smooth the iced aerofoil geometry in different levels. The coarse level may cause surface characteristics lost and aerodynamics performance prediction incorrect, though it provides an easy way to generate a high quality structure grid on smoothed iced aerofoil. On the other hand, unstructured grid is widely used in CFD researches for its good applicability on arbitrary shapes, but it needs more complex data structure to describe the grid and more calculation time in flow simulation.

In this study, a structure/unstructured hybrid grid generation method is developed for aiming at taking the advantages of structure and unstructured grids. The use of unstructured grid in this study aims at the surface preparation and the structured grid is used to save the storage and reduce the computational time. To illustrate the method developed in this study, the commercial transport jet main aerofoil (B757/767) and 145-m glaze ice shape are taken into account. The grid generation method is composed of three main steps (Fig. 1), which are described as follows.

1. Create an O-type single block structure grid with hyperbolic method on the clean aerofoil without ice shape. The grid points are equally distributed on the surface of aerofoil to make the grid smooth and uniformity. The far field boundary is taken as 10 chord lengths away from the aerofoil surface.
2. Inset the iced aerofoil at the same location where the clean aerofoil was located. Split the single block structure grid generated in step 1 into two parts according to the iced aerofoil and make sure that the inner part of the grid can envelope the whole iced aerofoil.
3. Delete the inner part of structure grid. Adjust and redistribute the point number to fit the iced aerofoil geometry well. Generate an unstructured grid in the empty zone between iced aerofoil surface and

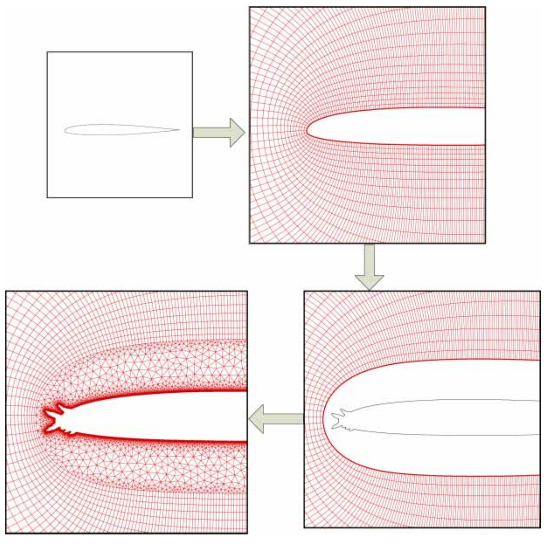

**Fig. 1** The process of generating a hybrid grid on complex iced aerofoil

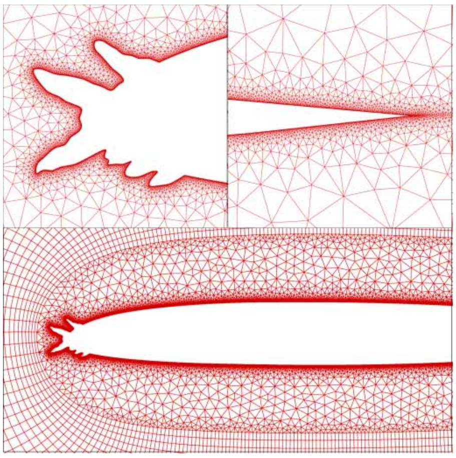

**Fig. 2** Hybrid grids on B757/767 aerofoil with 145-m ice

the structure grid. The outer boundary points of the unstructured grid are the same as boundary points of the first grid line of the structure grid.

With the method just described, the two blocks of grid are connected with each other at the interface in point-to-point type. It simplifies the disposal of flux construction at the interface between two different types of grid and keeps the most characteristics of iced aerofoil. The unstructured grid is only used in a smaller zone to reduce the total of the grid point. And there is no highly clustered grid line problem at the interface that may occur when generating a multi-block structure grid. Figure 2 shows the result of generating a hybrid grid on commercial transport jet main aerofoil (B757/767) with 145-m ice shape through using the method described above.

## 3 NUMERICAL METHOD

In this section, the numerical method used in this paper is discussed. At first, the Navier–Stokes equations are presented with their solution method. Then, the boundary conditions are discussed in brief.

### 3.1 Governing equation

The finite-volume method, which is based on the integral forms of Navier–Stokes equations, is widely used in CFD research for its good applicability to arbitrary geometry. The two-dimensional Reynolds-averaged Navier–Stokes equations can be presented in integral forms as follows

$$\frac{\partial}{\partial t}\int_{\Omega}\mathbf{Q}\,\mathrm{d}\Omega+\oint_{\partial\Omega}\mathbf{F}(x)\,\mathrm{d}y+\oint_{\partial\Omega}\mathbf{F}(y)\,\mathrm{d}x=0 \qquad (1)$$

where Ω is the control volume and the other parts of the equation are described as follows

$$\mathbf{Q}=\begin{bmatrix}\rho\\ \rho u\\ \rho v\\ \rho E\end{bmatrix},$$

$$\mathbf{F}(x)=\begin{bmatrix}\rho u\\ \rho u^2+p-\dfrac{M_\infty}{Re}\tau_{xx}\\ \rho uv-\dfrac{M_\infty}{Re}\tau_{yx}\\ \rho uH-\dfrac{M_\infty}{Re}\left(\tau_{xx}u+\tau_{xy}v+k\dfrac{\partial T}{\partial x}\right)\end{bmatrix},$$

$$\mathbf{F}(y)=\begin{bmatrix}\rho v\\ \rho uv-\dfrac{M_\infty}{Re}\tau_{xy}\\ \rho v^2+p-\dfrac{M_\infty}{Re}\tau_{yy}\\ \rho vH-\dfrac{M_\infty}{Re}(\tau_{yx}u+\tau_{yy}v+k\dfrac{\partial T}{\partial y})\end{bmatrix} \qquad (2)$$

The classical Jameson–Schmidt–Turkel (JST) [**6**, **7**] method with modified adaptive dissipation is used to solve the Navier–Stokes equations on both structure and unstructured grid. The fluxes at cell faces are interpolated by using arithmetic averaging of two neighbour cells' fluxes. To overcome divergence, a combination of second-order and fourth-order scalar dissipation terms is used. Time marching is completed by using an explicit method based on hybrid multi-stages method [**8**].

In most iced aerofoil flow field simulations [**9**, **10**], the Spalart–Allmaras (SA) one-equation turbulence model [**11**] is used to model the turbulence, but the two-equation shear-stress transport (SST) model of Menter [**12**] is selected to model turbulence as the main turbulence model in this paper. The SST turbulence model is more suitable for separated turbulence flow, which is similar to the flow passing around the iced aerofoil, comparing with one-equation turbulence model. All of the governing equations and the turbulence models are integrated to the wall, and no wall functions are used.

### 3.2 Boundary conditions

For hybrid grid used in this study, the boundary needs to be carefully treated at the interface between the two types of grid. The ghost cell method is used to simplify the implement of boundary conditions. There are two layers of ghost cells at the boundary of structured grid and one layer of ghost cells at the boundary of unstructured grid. The flow variables and geometry parameter of ghost cells are taken from the corresponding domain cells. The far field boundary condition is implemented at the outer boundary of structured grid, and no slip and adiabatic wall conditions are used at iced aerofoil surface.

## 4 RESULTS

The main purpose of this study is to assess how well the hybrid grid and numerical method can predict the aerodynamics performance of iced aerofoil. In validation calculation, the free stream Mach number is 0.29, static pressure is 94 121.6 Pa and static temperature is 261.55 K. The number of unstructured grid is 32 941 and the number of structure grid is 400 × 51. The angle of attack (AOA) simulated ranges from 0° to 11°, increasing 1° every step.

The lift, drag, and moment coefficients are calculated at various angles of attack to find the relationship between them and the lift coefficient is compared with the experiment, which can be found in reference [**3**], to validate the CFD program and the grid generation method. The drag and moment coefficients are not taken into comparison due to the lack of experimental data.

The lift coefficients at different AOA are described in Fig. 3. It is found that the lift coefficient of clean aerofoil is in agreement well with the experimental data and sample calculation validates the CFD program. The result also shows a good agreement between computational result and experimental data at low angles of attack for iced aerofoil. With the increasing of AOA, the computational result departs from the experimental data. For the ice accretion, the lift coefficient of iced aerofoil is smaller than the clean aerofoil at the same AOA. With the increasing of AOA, this characteristic is more evident. At 10° of AOA, the lift coefficient reduces about 30 per cent compared with the one of clean aerofoil. Due to the lack of experimental data, the stall angle cannot be judged directly. From the result of calculation, it is found that the stall phenomenon is not obvious even at 11° of AOA. But, at the same AOA, the flow is almost unsteady and there is large separated region on the upper surface of iced aerofoil, which is shown in the rest of this paper.

Figures 4 and 5 describe the drag coefficient and moment coefficient of computational result. The

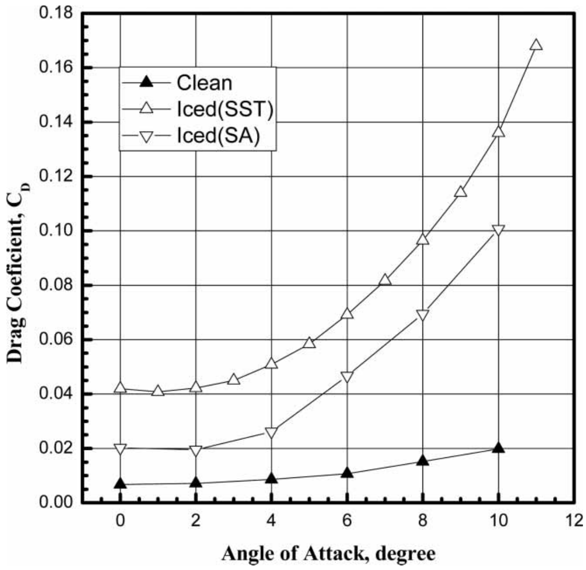


**Fig. 4** Drag coefficient of B757/767 aerofoil with 145-m ice

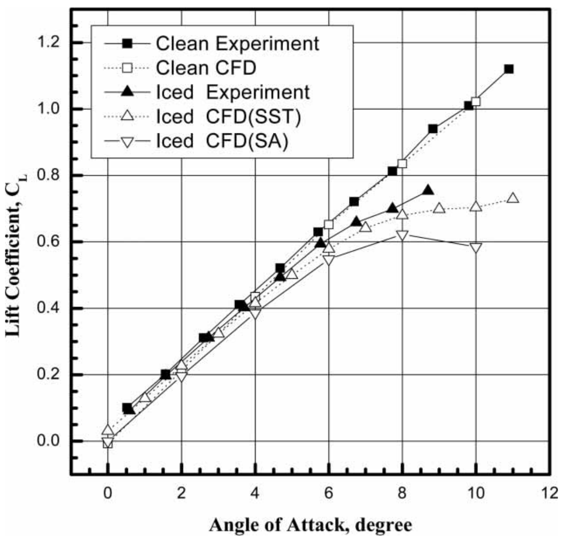


**Fig. 3** Lift coefficient of B757/767 aerofoil with 145-m ice

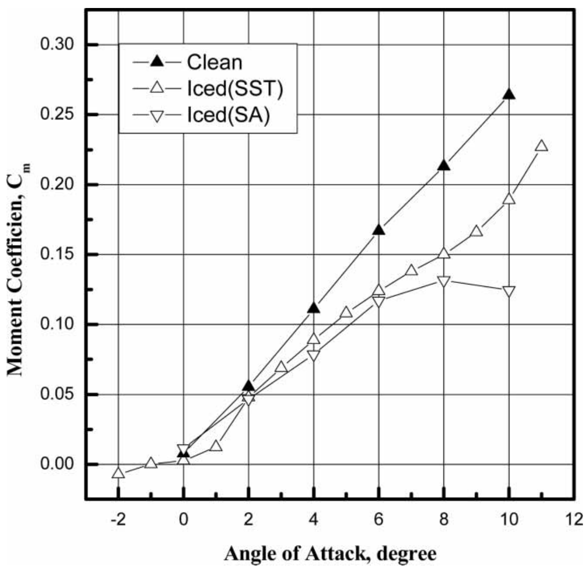


**Fig. 5** Moment coefficient of B757/767 aerofoil with 145-m ice

results show a sharp increase in drag coefficient when ice accretes at the leading edge of commercial transport jet main aerofoil (B757/767). The drag coefficient of iced aerofoil is bigger than clean aerofoil even at 0° of AOA. This is mainly because there are two large protruding horns at the leading edge of aerofoil. The trough formed by these two horns can block the flow. The drag coefficient increases about 575 per cent at 10° of AOA. The results also show a sharp non-linear departure in moment coefficient, when comparing with the result of clean aerofoil. This may cause demotion of control characteristics and damage the flight safety.

The contour and streamline results are also obtained by using the method described in this paper. Figures 6 to 8 are some results at typical angles of attack. As shown in Fig. 6, the vortex flow occurs behind the ice horns even at AOA = 0° and the influence region is larger at lower surface for the feather surface. With the increasing of AOA, the separated regions after the horns on aerofoil upper surface spread out whereas those after the horns on aerofoil lower surface reduce, which causes the lift to reduce and drag to increase. Figures 7 and 8 show the changes correctly. And the SST turbulence model acts properly to well model the separated flow passing the iced aerofoil.

To verify the effect of grid on the use of turbulence models, the SA one-equation turbulence model is also taken into account. The calculation results are shown in Fig. 4 through Fig. 7. From the results, it shows that the calculation result of lift coefficient is also in agreement with the experiment data at low AOA, but a little less prediction than the SST model. With the increasing of the AOA, the calculation result of SA model separates from the experiment data and predicts much lower lift coefficient than SST model, which also occurs on the calculation of drag coefficient and is more serious. And the stall AOA predicted with using the SA model is at about 8°, which does not occur in the experiment case. Both turbulence models predict the increase of drag coefficient correctly, but the SA model less predicts the drag coefficient than SST model. The moment coefficient result also shows that the ice accretion affects the aerodynamic characteristics seriously. And the non-linear departure is more serious with using SA model. The calculation results, especially the lift coefficient result, show that SA model is not very suitable for serious separated flow around iced aerofoil than SST model.

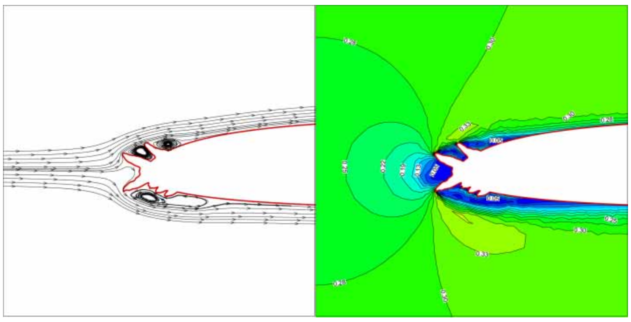

**Fig. 6** Mach contour and streamlines of 145-m iced aerofoil at AOA = 0°

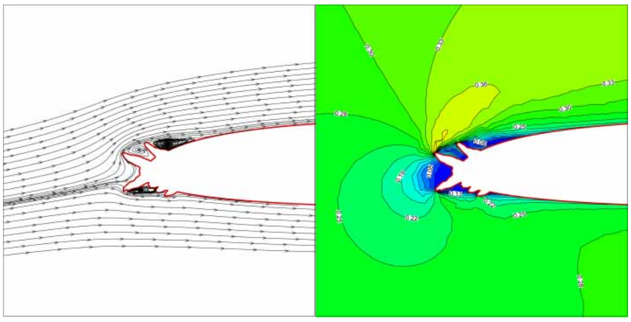

**Fig. 7** Mach contour and streamlines of 145-m iced aerofoil at AOA = 4°

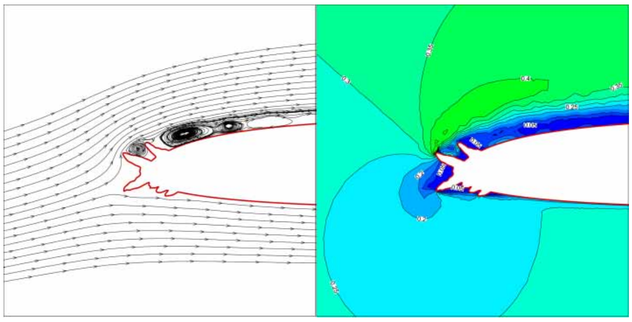

**Fig. 8** Mach contour and streamlines of 145-m iced aerofoil at AOA = 6°

## 5 CONCLUSION

In this paper, a structure/unstructured point-to-point multi-block hybrid grid generation method is developed. To validate the method, the commercial transport jet main aerofoil (B757/767) ice shape 145 m is selected in the study. In flow simulation, the JST method performs well in the study and the SST turbulence model shows good performance to simulate the separated flow around the iced aerofoil. At high AOA, the flow is almost unsteady and the flow is separated, even the SST turbulence model performs not very well. Finally, the computational results show quite good agreement with the experimental data in lift coefficient, which proves the efficiency of this method. And the drag and moment coefficient results show that the ice accretion degrades the aerodynamic performance of aerofoil.

## REFERENCES


1 **Chi, X., Zhu, B., Shih, T. I.-P., Slater, J. W., Addy, H. E.,** and **Choo, Y. K.** Computing aerodynamic performance of a 2D Iced airfoil: blocking topology and grid generation. AIAA paper 2002-0381, 2002.

2 **Vickerman, M. B., Choo, Y. K., Schilling, H. W., Braun, D. C., Baez, M.,** and **Cotten, B. J.** SmaggIce: further progress in software for gridding 2D iced airfoils. AIAA paper 2005-1369, 2005.

3 **Addy, H. E.** Ice accretions and icing effects for modern airfoils. NASA/TP 2000-210031, 2000.

4 **Zhu, B., Chi, X., Shih, T. I.-P.,** and **Slater, J. W.** Computing aerodynamic performance of 2D iced airfoils: blocking strategy and convergence rate. AIAA paper 2002-3049, 2002.

5 **Zhu, B., Chi, X., Shih, T. I.-P., Slater, J. W.,** and **Addy, H. E.** Computing aerodynamic performance of 2-D iced airfoils with structured grids. AIAA paper 2003-1071, 2003.

6 **Jameson, A., Schmidt, W.,** and **Turkel, E.** Numerical solutions of the Euler equations by finite volume methods using Runge–Kutta time-stepping schemes. AIAA paper 81-1259, 1981.

7 **Hdmes, D. G.** and **Connell S. D.** Solution of the 2D Navier–Stokes equations on unstructured adaptive meshes. AIAA paper 89-1932, 1989.

8 **Mavriplis, D. J.** and **Jameson, A.** Multigrid solution of the Navier–Stokes equations on triangular meshes. *AIAA J.*, 1990, **28**, 1415–1425.

9 **Chung, J., Choo, Y., Reehorst, A., Potapczuk, M.,** and **Slater, J.** Navier–Stokes analysis of the flowfield characteristics of an ice contaminated aircraft wing. AIAA paper 99-0375, 1999.

10 **Chung, J. J.** and **Addy, H. E.** A numerical evaluation of icing effects on a natural laminar flow airfoil. AIAA paper 2000-0096, 2000.

11 **Spalart, P. R.** and **Allmaras, S. R.** A one-equation turbulence model for aerodynamics flows. AIAA paper 92-0439, 1992.

12 **Menter, F. R.** Zonal two-equation $k$–$\omega$ turbulence models for aerodynamic flows. AIAA paper 93-2906, 1993.


## APPENDIX

### Notation

| | |
|---|---|
| $c$ | chord |
| $C_D$ | drag coefficient |
| $C_L$ | lift coefficient |
| $C_m$ | moment coefficient |
| $E$ | total energy |
| $F$ | convective and viscous flux |
| $H$ | total enthalpy |
| $k$ | heat conductivity |
| $M_\infty$ | free stream Mach number |
| $P$ | pressure |
| $\mathbf{Q}$ | state vector |
| $R_c$ | residual of convective term |
| $R_d$ | residual of dissipation term |
| $Re$ | Reynolds number |
| $T$ | temperature |
| $u$ | velocity in $x$-coordinate direction |
| $v$ | velocity in $y$-coordinate direction |
| $x$ | $x$-coordinate |
| $y$ | $y$-coordinate |
| | |
| $\alpha$ | Runge–Kutta coefficient |
| $\beta$ | split coefficient |
| $\Delta t$ | time step |
| $\tau$ | shearing stress |
| $\Omega$ | control volume |